

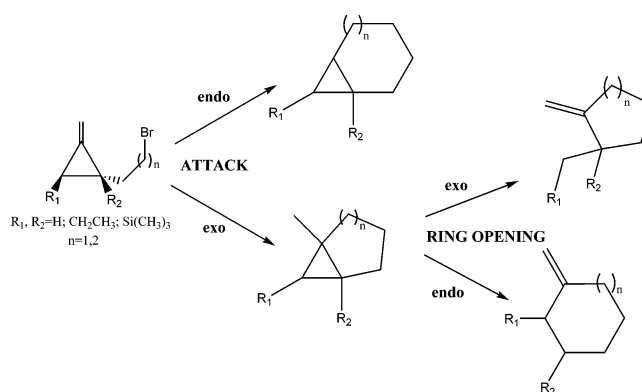
Radical Ring Expansion Reactions of Methylene-cyclopropane Derivatives: A Theoretical Study

Diego Ardura and Tomás L. Sordo*

Departamento de Química-Física y Analítica, Universidad de Oviedo, C/ Julián Clavería, 8, 33006 Oviedo, Spain

tsordo@uniovi.es

Received February 8, 2006



The evolution of the primary radicals from 1-(3-bromopropyl)-2-ethyl-3-methylene-cyclopropane, 1-(3-bromopropyl)-1-trimethylsilyl-2-methylene-cyclopropane, 1-(3-bromobutyl)-2-ethyl-3-methylene-cyclopropane, and 1-(3-bromobutyl)-1-trimethylsilyl-2-methylene-cyclopropane was theoretically studied at the ROMP2/6-311++G(d,p)/UB3LYP/6-31G(d,p) theory level taking into account the effect of solvent through a PCM-UAHF model. For the propyl-substituted radicals, the attack of the radical center on the double bond takes place most favorably in an exo fashion. The subsequent ring expansions yield the product corresponding to the rupture of the endo C–C bond as the most favorable one in accordance with the experimental results. In the case of 1-(3-bromobutyl)-2-ethyl-3-methylene-cyclopropane, the Gibbs energy barriers for the endo and exo attacks are the same, and the subsequent reversible evolution yields the product corresponding to the rupture of the exo C–C bond as the most favorable one through thermodynamic control in agreement with experiment. Finally, for 1-(3-bromobutyl)-1-trimethylsilyl-2-methylene-cyclopropane, our calculations predict that the endo attack is 0.8 kcal/mol more favorable than the exo one. In the subsequent reversible ring expansion, the product corresponding to the rupture of the endo C–C bond is kinetically the most favored one in reasonable agreement with the experimental observations.

Introduction

Radical ring expansion reactions are extremely useful processes that take advantage of existing ring structures for the construction of larger cyclic systems.¹ Among these processes, ring opening of the cyclopropylcarbinyl radical has been proved

to be a useful strategy for ring expansion.² In an interesting extension, Destabel and Kilburn³ have described the ring expansion of 1-(3-bromopropyl)-2-methylene-cyclopropane **1** where the tin hydride treatment resulted in 1,5-addition of the radical to the exocyclic double bond. This was followed by ring opening of the cyclopropylcarbinyl radical, yielding methylene-cyclohexane **2** (see Scheme 1).

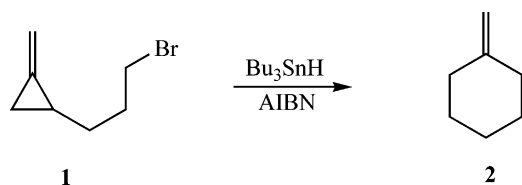
* To whom correspondence should be addressed. Phone: +34 98 5 103 475. Fax: +34 98 5 103 1255.

(1) Hesse, M. *Ring Enlargement in Organic Chemistry*; VCH: Weinheim, 1991.

(2) Dowd, P.; Zhang, W. *Chem. Rev.* **1993**, *93*, 2091–2115.

(3) Destabel, C.; Kilburn, J. D. *J. Chem. Soc., Chem. Commun.* **1992**, 596–598.

SCHEME 1



Further studies of methylenecyclopropane⁴ derivatives have shown that cyclization of (methylenecyclopropyl)propyl radicals from bromides **3** and **5** (see Scheme 2) gave methylenecyclohexane products **4** and **6** via initial 5-exo cyclization followed by ring opening of the cyclopropyl methyl radical.

The cyclization of a (methylenecyclopropyl)butyl radical from **7** led to a 1:1 mixture of products **9** and **10** which result from initial 6-exo and 7-endo cyclization, respectively, along with reduced uncyclized **8**. However, cyclization of silyl radical **11** proceeds predominantly in a 7-endo fashion to give the bicyclo 1.5.0 octane **14** and also to give moderate amounts of the directly reduced product **12** with smaller amounts of methylenecycloheptane **13** obtained from initial 6-exo cyclization.

The addition of carbon-centered radicals to C=C double bonds is an important carbon-carbon bond forming process and has been investigated both experimentally and theoretically.⁵ The reaction is generally exothermic because a π bond is replaced by a σ bond. Therefore, according to Hammond's postulate,⁶ the transition state (TS) bears an early character. As stated by Baldwin's rules,⁷ the preference between the exo or endo attack of a radical atom on a double bond is determined

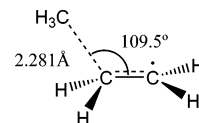
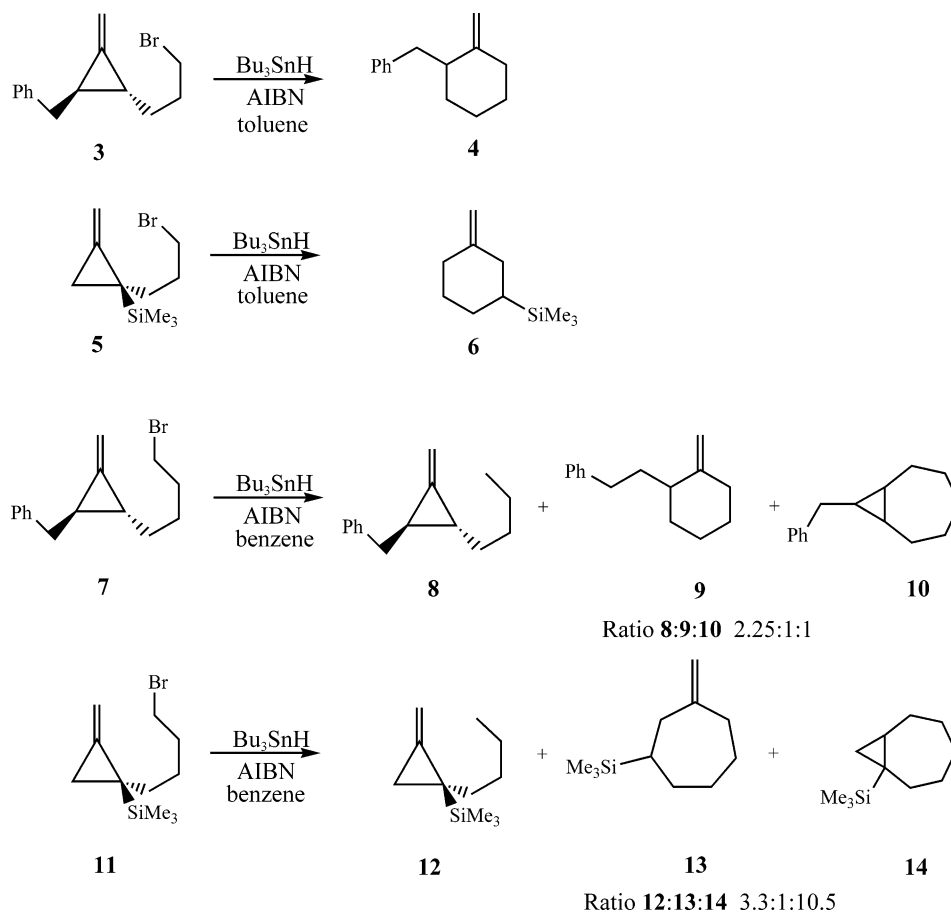


FIGURE 1. Transition structure for the addition of the methyl radical to ethene (QCISD(T)/6-31G(d)).^{5d}

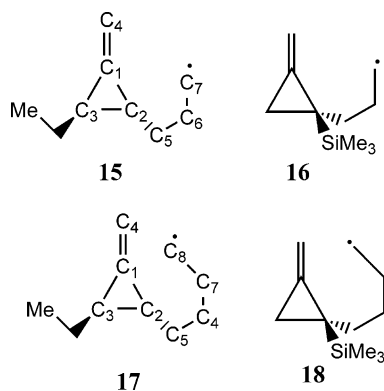
by the stereochemical requirements of the transition states for the ring closure processes. The most favored ring closures are those in which the length and the nature of the linking chain enable the terminal atoms to achieve the required trajectories to form the final ring bond. The addition of the radical carbon atom to the double bond corresponds to a trigonal ring closure process where the optimum angle of approach is 109°. In agreement with this, high-level calculations on the attack of a methyl radical to a double bond^{5d,8} have shown that at the TS the forming bond is still long (2.281 Å), but the angle of attack (109.5°) is already close to the corresponding angle in the product radical (see Figure 1).

In the present paper, we report a theoretical study of the radical ring expansions of the primary radicals from 1-(3-bromopropyl)-2-ethyl-3-methylenecyclopropane, **15**, 1-(3-bromopropyl)-2-methylene-1-trimethylsilylcyclopropane, **16**, 1-(4-bromobutyl)-2-ethyl-3-methylenecyclopropane, **17**, and 1-(4-bromobutyl)-2-methylene-1-trimethylsilylcyclopropane, **18** (see Scheme 3) as model systems of **3**, **5**, **7**, and **11** in Scheme 2. The radical intramolecular attack on the double bond and the subsequent evolution of the bicyclic compounds formed in this first step will be analyzed by taking into account the effect of solvent.

SCHEME 2



SCHEME 3



Methods

Quantum chemical computations were performed using the Gaussian 98 series of programs.⁹ The geometries of the stable species and TSs were fully optimized in the gas phase at the UB3LYP/6-31G(d,p) theory level¹⁰ using Schlegel's algorithm.¹¹ Harmonic vibrational frequencies were also calculated at the UB3LYP/6-31G(d,p) theory level to characterize the critical points and to evaluate the zero-point vibrational energy (ZPVE). Single-point calculations were also performed in the gas phase on the UB3LYP/6-31G(d,p) optimized geometries at the ROMP2/6-311++G(d,p) level.¹² An NBO population analysis¹³ was performed at the UB3LYP/6-311++G(d,p)/UB3LYP/6-31G(d,p) level. ΔG values were computed in the gas phase using the UB3LYP/6-31G(d,p) frequencies within the ideal gas, rigid rotor, and harmonic oscillator approximations¹⁴ at 1 atm and 353.15 K which were the experimental conditions. To take into account condensed-phase effects, we used a self-consistent reaction-field (SCRF) model proposed for quantum chemical computations on solvated molecules.^{15–17} In this model, the solvent is represented by a dielectric

continuum characterized by its relative static dielectric permittivity ϵ . The solute, which is placed in a cavity created in the continuum after spending some cavitation energy, polarizes the continuum, which in turn creates an electric field inside the cavity. This interaction can be taken into account using quantum chemical methods by minimizing the electronic energy of the solute plus the Gibbs energy change corresponding to the solvation process. Addition to ΔG_{gas} of the solvation Gibbs energy gives $\Delta G_{\text{solution}}$.

To calculate the electrostatic potential created by the polarized continuum in the cavity, we employed the polarizable continuum model (PCM) with the united atom Hartree–Fock (UAHF) parametrization.¹⁸ The solvation Gibbs energies, $\Delta G_{\text{solvation}}$, along the reaction coordinates were evaluated from single-point PCM calculations on the gas-phase optimized geometries at the UB3LYP/6-311++G(d,p) theory level. A relative permittivity of 2.247 was employed to simulate benzene as solvent.

Computational Results

We will present first the results obtained for the cyclization of the primary radicals **15** and its silylated derivative **16**, and then we will present the results for the cyclization of the primary radicals **17** and **18**. Tables 1S–4S in the Supporting Information collect the energies of all the critical structures located along the reaction coordinates. Figures 2–5 display the corresponding ROMP2/6-311++G(d,p)/UB3LYP/6-31G(d,p) Gibbs energy profiles in solution. Tables 5S–8S of the Supporting Information collect the absolute electronic energies and ZPVEs, and Tables 10S and 11S collect the most important NBO atomic spin densities. Table 25S (Supporting Information) collects the Cartesian coordinates of all the critical structures located. Figures 1S–4S (Supporting Information) show the optimized geometries of all the critical structures. Atom numbering is displayed in Scheme 3. Unless otherwise stated, relative ROMP2/6-311++G(d,p)/UB3LYP/6-31G(d,p) Gibbs energies in solution will be discussed in the text.

Evolution of the Primary Radical from 1-(3-Bromopropyl)-2-ethyl-3-methylene-cyclopropane. According to our theoretical results, the primary radical **15**, **R-p**, in which the unpaired electron is localized at C7 (total NBO spin density = +1.005), initially undertakes a conformational change through TS **TSR1-p** (4.3 kcal/mol) to yield the appropriate intermediate **M1-p** (0.7 kcal/mol) for cyclization (see Figure 2). **M1-p** can evolve through two different routes. The first one corresponds to a 6-endo cyclization through the TS **TS1P1-p** with an energy barrier of 14.2 kcal/mol for the nucleophilic attack of the radical carbon atom C7 on the C4 carbon atom of the methylene moiety to form the bicyclic product **P1-p** (−20.8 kcal/mol). At **TS1P1-p**, the attacking distance (C4–C7) is 2.370 Å and the α unpaired spin is distributed mainly between C1 (+0.346) and C7 (+0.783); C4 presents a small spin polarization of −0.169. The angle of approach of the radical to the double bond is 96.0°. At **P1-p**, the C4–C7 distance is 1.553 Å and the α unpaired spin is located mainly at C1 (+0.875).

The second route proceeds via a 5-exo cyclization through TS **TS12-p** with an energy barrier of 10.0 kcal/mol for the attack of the radical carbon atom C7 on the carbon atom C1 of the cyclopropane ring to yield the bicyclic intermediate **M2-p** (−31.8 kcal/mol). At **TS12-p**, the attacking distance (C1–C7) is 2.362 Å, and the angle of approach of the radical to the double bond is 107.8°. Also, the spin density is mainly distributed between C4 (+0.395) and C7 (+0.781), and C1 presents a slight spin polariza-

(4) Destabel, C.; Kilburn, J. D.; Knight, J. *Tetrahedron Lett.* **1993**, *34*, 3151–3154.

(5) See, for example: (a) Giese, B. *Radicals in Organic Syntheses: Formation of Carbon–Carbon Bonds*; Pergamon: Oxford, 1986. (b) Curran, D. P. In *Comprehensive Organic Synthesis*; Trost, B. M., Fleming, I. M., Semmelhack, M. F., Eds.; Pergamon: Oxford, 1991; Vol. 4. (c) Fossey, J.; Lefort, D.; Sorba, J. *Free Radicals in Organic Chemistry*; Wiley: New York, 1995. (d) Fischer, H.; Radom, L. *Angew. Chem., Int. Ed.* **2001**, *40*, 1340–1371. (e) Henry, D. J.; Coote, M. L.; Gómez-Balderas, R.; Radom, L. *J. Am. Chem. Soc.* **2004**, *126* (6), 1732–1740.

(6) Hammond, D. S. *J. Am. Chem. Soc.* **1955**, *77*, 334–338.

(7) Baldwin, J. E.; *J. Chem. Soc., Chem. Commun.* **1976**, 734–736.

(8) Wong, M. W.; Radom, L. *J. Phys. Chem.* **1995**, *99*, 8582–8585.

(9) Frisch, M. J.; Trucks, G. W.; Schlegel, H. B.; Scuseria, G. E.; Robb, M. A.; Cheeseman, J. R.; Zakrzewski, V. G.; Montgomery, J. A., Jr.; Stratmann, R. E.; Burant, J. C.; Dapprich, S.; Millam, J. M.; Daniels, A. D.; Kudin, K. N.; Strain, M. C.; Farkas, O.; Tomasi, J.; Barone, V.; Cossi, M.; Cammi, R.; Mennucci, B.; Pomelli, C.; Adamo, C.; Clifford, S.; Ochterski, J.; Petersson, G. A.; Ayala, P. Y.; Cui, Q.; Morokuma, K.; Malick, D. K.; Rabuck, A. D.; Raghavachari, K.; Foresman, J. B.; Cioslowski, J.; Ortiz, J. V.; Stefanov, B. B.; Liu, G.; Liashenko, A.; Piskorz, P.; Komaromi, I.; Gomperts, R.; Martin, R. L.; Fox, D. J.; Keith, T.; Al-Laham, M. A.; Peng, C. Y.; Nanayakkara, A.; Gonzalez, C.; Challacombe, M.; Gill, P. M. W.; Johnson, B. G.; Chen, W.; Wong, M. W.; Andres, J. L.; Head-Gordon, M.; Replogle, E. S.; Pople, J. A. *Gaussian 98*; Gaussian, Inc.: Pittsburgh, PA, 1998.

(10) (a) Becke, A. D. *Phys. Rev. A* **1988**, *38*, 3098–3100. (b) Lee, C.; Yang, W.; Parr, R. G. *Phys. Rev. B* **1988**, *37*, 785–789. (c) Becke, A. D. *J. Chem. Phys.* **1993**, *98*, 5648–5652.

(11) Schlegel, H. B. *J. Comput. Chem.* **1982**, *3*, 214–218.

(12) Hehre, W. J.; Radom, L.; Pople, J. A.; Schleyer, P. v. R. *Ab Initio Molecular Orbital Theory*; John Wiley & Sons Inc.: New York, 1986.

(13) Reed, A. E.; Curtiss, L. A.; Weinhold, F. *Chem. Rev.* **1988**, *88*, 899–926.

(14) McQuarrie, D. A. *Statistical Mechanics*; Harper & Row: New York, 1976.

(15) Rivalet, J. L.; Rinaldi, D.; Ruiz-López, M. F. In *Theoretical and Computational Model for Organic Chemistry*; Formosinho, S. J., Csizmadia, I. G., Arnaut, L., Eds.; NATO ASI Ser. C; Kluwer Academic Publishers: Dordrecht, 1991; Vol. 339, pp 79–92.

(16) (a) Tomasi, J.; Persico, M. *Chem. Rev.* **1994**, *94*, 2027–2094. (b) Cammi, R.; Tomasi, J. *J. Comput. Chem.* **1995**, *16*, 1449–1458.

(17) Cramer, C. J.; Truhlar, D. G. *Chem. Rev.* **1999**, *99*, 2161–2200.

(18) Barone, V.; Cossi, M.; Tomasi, J. *J. Chem. Phys.* **1997**, *107*, 3210–3221.

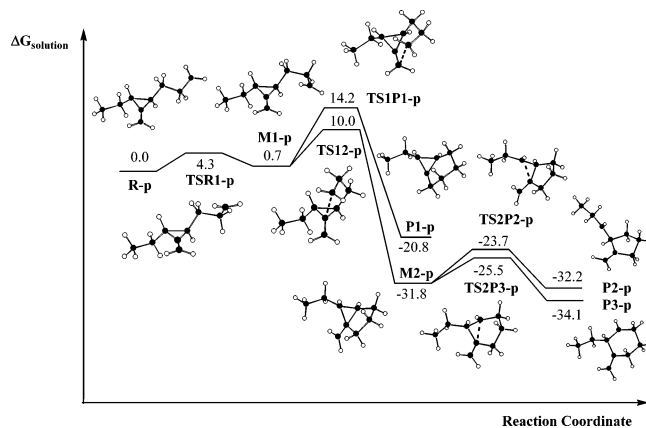


FIGURE 2. ROMP2 Gibbs energy profiles (kcal/mol) in solution for the evolution of the primary radical from 1-(3-bromopropyl)-2-ethyl-3-methylenecyclopropane.

tion (−0.159). At **M2-p**, the C1–C7 distance is 1.543 Å and the spin density is localized at C2 (+0.121) and C4 (+0.914). **M2-p** can further evolve in two different ways. The first one corresponds to an exo ring opening through the TS **TS2P2-p** for the C1–C3 bond breaking with an energy barrier of 8.1 kcal/mol to give the cyclopentane derivative **P2-p** (−32.2 kcal/mol). At **TS2P2-p**, the α spin density is distributed between C3 (+0.537) and C4 (+0.592), with C1 presenting some spin polarization (−0.129). The second route proceeds through **TS2P3-p** with an energy barrier of 6.3 kcal/mol for the endo ring opening of bicyclic **M2-p** through the C1–C2 bond breaking to yield the six-membered ring **P3-p** (−34.1 kcal/mol). At **TS2P3-p**, the α spin density is localized at C2 (+0.546) and C4 (+0.586), and C1 presents spin polarization (−0.129). It is interesting to note that the theoretical Gibbs energy profiles in solution indicate that the two ring opening processes from **M2-p** are reversible (see Figure 2) so that the predicted **P3-p**:**P2-p** ratio would be determined by the energy difference between those products through thermodynamic control. Therefore, according to our computational results, the major product from 1-(3-bromopropyl)-2-ethyl-3-methylenecyclopropane would be the endo product, **P3-p**, which is 1.9 kcal/mol more stable than the exo one, **P2-p**, in agreement with experimental findings.

To assess the adequacy of the theoretical methods employed by us to obtain the above-displayed energy profiles, we performed single-point calculations on the B3LYP optimized geometries along the reaction coordinate for the evolution of the primary radical from 1-(3-bromopropyl)-2-ethyl-3-methylenecyclopropane at the CCSD(T)/6-31G(d,p) theory level. In Table 1, we compare the relative electronic energies obtained at the B3LYP/6-31G(d,p), ROMP2/6-31G(d,p)//B3LYP/6-31G(d,p), and CCSD(T)/6-31G(d,p)//B3LYP/6-31G(d,p) theory levels. From Table 1, we can see that the ROMP2//B3LYP energy profile is in reasonable agreement with

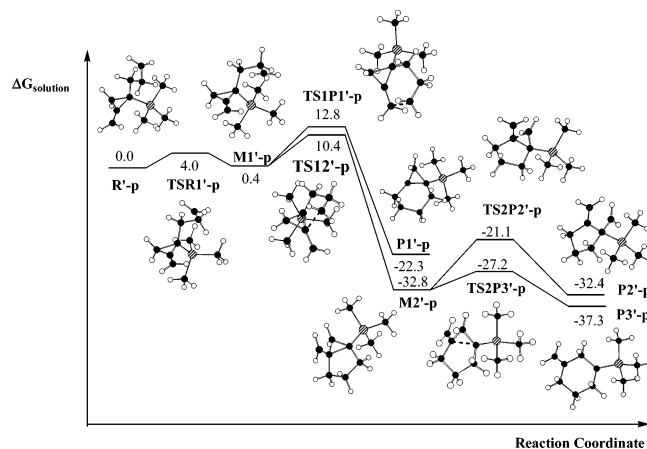


FIGURE 3. ROMP2 Gibbs energy profiles (kcal/mol) in solution for the evolution of the primary radical from 1-(3-bromopropyl)-1-trimethylsilyl-2-methylenecyclopropane.

the CCSD(T)//B3LYP one. Both theory levels render the TS **TS12-p** as the rate-determining one with practically the same energy barrier. Therefore, we will employ the ROMP2//B3LYP theory level in the study of the larger systems in the three following sections.

Evolution of the Primary Radical from 1-(3-Bromopropyl)-1-trimethylsilyl-2-methylenecyclopropane. The mechanism for the cyclization of the primary radical **16**, **R'-p**, is analogous to that found for **15** (see Figure 3). The energy barriers corresponding to **TS1P1'-p** for the 6-endo cyclization (12.8 kcal/mol) and to **TS12'-p** for the 5-exo cyclization (10.4 kcal/mol) are, respectively, 1.4 kcal/mol lower and 0.4 kcal/mol higher than those corresponding to the TSs for the analogous cyclizations in the primary radical **15** (**TS1P1-p** and **TS12-p**). Spin densities are now practically identical to those corresponding to the previous case (see Table 10S, Supporting Information). The angles of approach for the endo (**TS1P1'-p**) and exo (**TS12'-p**) attacks of the radical atom are now 104.0° and 106.0°, respectively. Along the 5-exo cyclization, **TS12'-p** renders the intermediate **M2'-p** (−32.8 kcal/mol) which in turn can undertake either an exo ring opening through **TS2P2'-p** (energy barrier = 11.7 kcal/mol) to give the cyclopentane derivative **P2'-p** (−32.4 kcal/mol) or an endo ring opening through the TS **TS2P3'-p** (energy barrier = 5.6 kcal/mol) to give the six-membered ring **P3'-p** (−37.3 kcal/mol).

Therefore, for **16**, computations render the endo product **P3'-p** 4.9 kcal/mol more stable and 6.1 kcal/mol kinetically more favorable than **P2'-p**. Consequently, **P3'-p** would be the unique product through kinetic control in agreement with the experimental results.

Evolution of the Primary Radical from 1-(4-Bromobutyl)-2-ethyl-3-methylenecyclopropane. The Gibbs free energy profile in solution for the evolution of the primary radical **17**, **R-b**, is parallel

TABLE 1. UB3LYP/6-31G(d,p), ROMP2/6-311++G(d,p)//UB3LYP/6-31G(d,p), and CCSD(T)/6-31G(d,p)//UB3LYP/6-31G(d,p) Relative Energies for the Evolution of the Primary Radical from 1-(3-Bromopropyl)-2-ethyl-3-methylenecyclopropane

structures	UB3LYP/6-31G(d,p)	ROMP2/6-311++G(d,p)// UB3LYP/6-31G(d,p)	CCSD(T)/6-31G(d,p)// UB3LYP/6-31G(d,p)
R-p	0.0	0.0	0.0
TSR1-p	3.3	3.2	3.3
M1-p	0.5	0.3	0.2
TS1P1-p	11.8	12.3	12.5
P1-p	−22.8	−25.4	−25.7
TS12-p	7.8	7.6	7.5
M2-p	−28.5	−35.8	−33.1
TS2P2-p	−20.9	−27.4	−22.7
P2-p	−31.8	−33.5	−34.0
TS2P3-p	−23.1	−29.6	−25.2
P3-p	−34.6	−38.0	−38.1

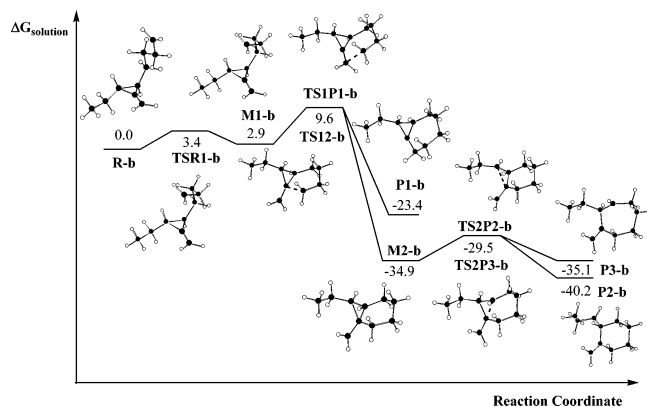


FIGURE 4. ROMP2 Gibbs energy profiles (kcal/mol) in solution for the evolution of the primary radical from 1-(4-bromobutyl)-2-ethyl-3-methylene-cyclopropane.

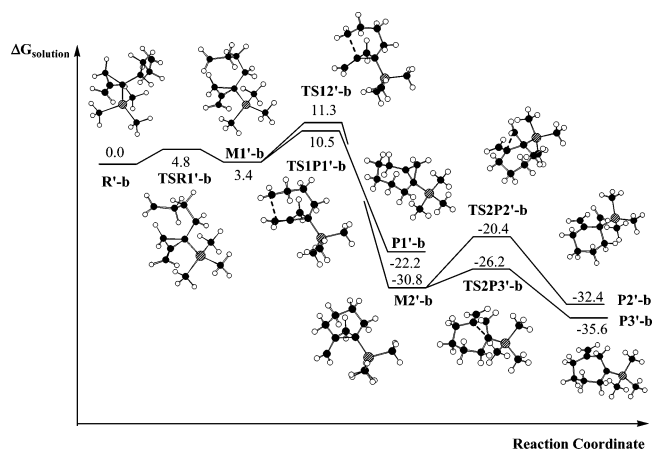


FIGURE 5. ROMP2 Gibbs energy profiles (kcal/mol) in solution for the evolution of the primary radical from 1-(4-bromobutyl)-1-trimethylsilyl-2-methylene-cyclopropane.

to those described before (see Figure 4). Here, the first two TSs for both the 7-endo and the 6-exo cyclizations, **TS1P1-b** and **TS12-b**, are competitive, presenting the same Gibbs free energy barrier in solution (9.6 kcal/mol). The angles of approach of the radical center C8 to the double bond in these two TSs are 102.2° and 102.8°, respectively.

Spin densities are analogous to those for the two previous reactions (see Table 11S, Supporting Information). Along the 7-endo pathway, the bicyclic product **P1-b** (−23.4 kcal/mol) is formed through the TS **TS1P1-b** whereas the evolution through **TS12-b** for 6-exo cyclization gives the intermediate **M2-b** (−34.9 kcal/mol). **M2-b** can evolve through two different TSs, **TS2P2-b** and **TS2P3-b**, with the same energy barrier (5.4 kcal/mol) to yield **P2-b** (−40.2 kcal/mol) and **P3-b** (−35.1 kcal/mol) products through exo and endo ring openings, respectively. As we see from Figure 4, the two ring opening processes from **M2-b** are reversible so that although they present the same energy barrier the resulting **P2-b**:**P3-b** ratio would be determined by the relative stability of these products through thermodynamic control. Therefore, as the energy barriers associated with **TS1P1-b** and **TS12-b** are the same and **P2-b** is 5.1 kcal/mol more stable than **P3-b**, our results predict that, from **17**, **P1-b** and **P2-b** would be obtained as a 1:1 mixture in agreement with experiment.

Evolution of the Primary Radical from 1-(4-Bromobutyl)-1-trimethylsilyl-2-methylene-cyclopropane. In light of our theoretical results, the evolution of the primary radical **18**, **R'-b**, is analogous to the profiles described above (see Figure 5). Initially, two different routes are possible corresponding to the 7-endo and 6-exo cycliza-

tions through **TS1P1'-b** (energy barrier = 10.5 kcal/mol) and **TS12'-b** (energy barrier = 11.3 kcal/mol) where the angles of approach of the radical atom C8 to the double bond are 102.5° and 100.1°, respectively. Along the 7-endo pathway, **TS1P1'-b** yields the bicyclic product **P1'-b** (−22.2 kcal/mol). The TS for the 6-exo attack, **TS12'-b**, yields an intermediate **M2'-b** (−30.8 kcal/mol) for which two different ring openings are possible. The first one corresponds to the exo ring opening through **TS2P2'-b** (energy barrier = 10.4 kcal/mol) for C1–C3 bond breaking to give the product **P2'-b** (−32.4 kcal/mol). The second one takes place in an endo fashion through **TS2P3'-b** (energy barrier = 4.6 kcal/mol) for C1–C2 bond breaking yielding **P3'-b** (−35.6 kcal/mol). Consequently, **P3'-b** would be the unique product obtained from **M2'-b** by kinetic control. Therefore, our theoretical results are in good agreement with the experimentally observed 1:10.5 mixture of **P3'-b** and **P1'-b**.

Discussion

We commented above about the reasonable agreement between the results obtained at the levels ROMP2//B3LYP and CCSD(T)//B3LYP. The largest discrepancy between the electronic energies obtained at these two levels corresponds to the TSs **TS2P2-p** and **TS2P3-p**. In an NBO analysis, we found that in these two structures there is an important interaction (second-order perturbation energy of interaction of about 40 kcal/mol) between the unpaired electron and the antibonding corresponding to the C–C ring bond which is breaking to open the three-membered cycle. This electronic rearrangement causing the ring opening gives the breaking C–C bond a three-electron-bond character which is better described at the CCSD(T)/6-31G(d,p) level. It is also interesting to note that despite the difference between the B3LYP and the ROMP2 energies obtained both methods display the same qualitative trends. These two methods render the same favored products, although in the cases of **15** and **17** the quantitative ratio of products experimentally observed is not as well reproduced with the B3LYP method as with the MP2 one.

The solvent effect is moderate and, in general, stabilizes the critical structures along the reaction coordinates, 0.1–2.7 kcal/mol, with respect to reactants (**TSR1-p** and **TSR1-b** become 0.2 and 0.3 kcal/mol destabilized by solvent, respectively, and **M1-b**, **TSR1'-b**, and **MI'-b** present no net solvent effect with respect to reactants).

For the cyclization of the primary radicals **15** and its silylated derivative, the values of the attack angle are closer to 109° in the more stable TSs as predicted by Baldwin's rules. However, for the butyl-substituted primary radicals, the greater length of the attacking chain gives rise to TSs with an earlier character and with values of the attack angles close to 102°.

To discuss the effect of ethyl and trimethylsilyl substituents, we have located the TSs for the initial attack and the subsequent ring opening along the evolution of the primary radicals from 1-(3-bromopropyl)-2-methylene-cyclopropane (**PMCP**) and from 1-(4-bromobutyl)-2-methylene-cyclopropane (**BMCP**) without substituents and with the ethyl and trimethylsilyl substituents interchanged (see Table 2). In the absence of ethyl or trimethylsilyl substituents, the exo attack is more favorable than the endo one by 4.4 kcal/mol in electronic energy for **PMCP** owing to the shortness of the propyl side chain. In the case of **BMCP**, however, both endo and exo attacks present similar electronic energy barriers because the butyl side chain is long enough to reach both the C1 and C4 atoms. For **PMCP**, on the other hand, the endo ring opening is favored over the exo one by 4.9 kcal/

TABLE 2. ROMP2/6-311++G(d,p)//UB3LYP/6-31G(d,p) Electronic Energies Corresponding to the TSs for the Initial Attack and the Subsequent Ring Opening along the Evolution of the Primary Radicals from 1-(3-Bromopropyl)-2-methylenecyclopropane and from 1-(4-Bromobutyl)-2-methylenecyclopropane without Substituents and with Ethyl and Trimethylsilyl Substituents on C2 and C3

ATTACK					
R	0.0	0.0	0.0	0.0	0.0
TS1P1 (endo)	12.4	12.3	12.5	10.1	11.6
TS12 (exo)	8.0	7.6	8.2	7.5	9.6
RING OPENING					
M2	-36.5	-35.8	-33.6	-38.3	-35.4
TS2P2 (exo)	-25.3	-27.4	-26.8	-26.9	-22.5
TS2P3 (endo)	-30.2	-29.3	-24.3	-32.1	-29.9
ATTACK					
R	0.0	0.0	0.0	0.0	0.0
TS1P1 (endo)	8.1	7.9	8.0	8.5	8.6
TS12 (exo)	8.0	7.3	8.3	8.2	9.2
RING OPENING					
M2	-39.3	-39.1	-36.8	-37.7	-34.7
TS2P2 (exo)	-31.8	-33.8	-31.7	-29.7	-24.6
TS2P3 (endo)	-33.0	-34.1	-28.7	-32.3	-30.3

mol because it yields a secondary radical and a six-membered cycle practically without ring strain. For **BMCP**, the endo ring opening is favored only by 1.2 kcal/mol because it renders a secondary radical with a strained seven-membered cyclic structure.

The presence of a substituent on C3 does not exert an appreciable influence on the initial attack but favors the exo ring opening because now the product is a secondary radical. With an ethyl substituent, this effect reduces the difference between endo and exo energy barriers to 1.9 and 0.3 kcal/mol for **PMCP** and **BMCP**, respectively, with the endo ring openings still being the more favorable ones. The effect of a trimethylsilyl substituent on C3 is much stronger because the electronic delocalization produced by its interaction with the singly occupied p orbital through hyperconjugation is larger. Thus, the exo ring openings become the more favorable ones for both **PMCP** and **BMCP** by 2.5 and 3.0 kcal/mol, respectively. On the other hand, a substituent on C2 produces two effects, which are stronger for the trimethylsilyl substituent than for the ethyl one. First, it reduces the angle between the C2–C5 bond and the ring plane (*gem*-effect), facilitating in this way the endo attack (this angle has a value of 126.3°, 120.0°, 130.3°, and 125.0° in **15**, **16**, **17**, and **18**, respectively, whereas the reduction of this angle is about 3° lower when the trimethylsilyl is replaced by an ethyl group). Second, it stabilizes the radical product formed by endo ring opening. The first effect is larger for the shorter side chain. Thus, the difference in the electronic

energy barrier favoring the exo attack reduces to 2.6 and 2.0 kcal/mol for **PMCP** with an ethyl and a trimethylsilyl substituent, respectively. For **BMCP**, the ethyl substituent favors the exo attack by 0.3 kcal/mol, but the trimethylsilyl substituent favors the endo attack by 0.6 kcal/mol in electronic energy. For **PMCP**, the endo ring opening, which renders an unstrained six-membered cyclic product, is 5.2 and 7.4 kcal/mol more favorable than the exo one with an ethyl or a trimethylsilyl on C2, respectively. For **BMCP**, the endo ring opening yields a strained seven-membered cyclic product and is only 2.6 and 5.7 kcal/mol more favorable than the exo one with an ethyl or a trimethylsilyl substituent on C2, respectively.

In summary, according to ROMP2/6-311++G(d,p)//UB3LYP/6-31G(d,p) calculations taking into account the effect of solvent through a PCM-UAHF model for 1-(3-bromopropyl)-2-ethyl-3-methylenecyclopropane and 1-(3-bromopropyl)-1-trimethylsilyl-2-methylenecyclopropane, the attack of the radical center C7 on the double bond takes place most favorably in an exo fashion. The subsequent ring expansions are reversible processes yielding the product corresponding to the rupture of the exo C–C bond as the most favorable one thus explaining the experimental results by thermodynamic control. In the case of 1-(4-bromobutyl)-2-ethyl-3-methylenecyclopropane, the Gibbs energy barriers for the endo and exo attacks are the same and the subsequent reversible evolution yields the product corresponding to the rupture of the endo C–C bond as the most favorable one. As a consequence, a 1:1 mixture of **P1-b** and

P2-b cyclization products is predicted by calculations through thermodynamically controlled ring expansion in agreement with experiment. Finally, for 1-(4-bromobutyl)-1-trimethylsilyl-2-methylene-cyclopropane, our calculations predict that the endo attack is 0.7 kcal/mol more favorable than the exo one. In the subsequent reversible ring expansion, the product corresponding to the rupture of the endo C–C bond is the most favorable one. Therefore, our theoretical results, through kinetically controlled ring expansion, are in reasonable agreement with the 1:10.5 ratio found in the experimental work.

Supporting Information Available: Structures, absolute electronic energies, ZPVEs, relative electronic energies, relative ZPVEs, relative Gibbs energies in the gas phase, relative Gibbs energies of solvation, relative Gibbs energies in solution, imaginary frequencies of the TSs, Cartesian coordinates, and most important NBO spin densities of the critical structures located along the reaction paths. This material is available free of charge via the Internet at <http://pubs.acs.org>.

JO0602625